Gravity gradiometer design comparison by three different methods

James Brewster*
Bell Geospace, Inc
Houston, TX, USA
jbrewster@bellgeo.com

*presenting author asterisked

SUMMARY

Two gravity gradiometer designs are currently available for commercial survey operations and other instruments are in the late stages of pre-deployment research. These gradiometer systems differ from one another with respect to the number and orientation of sensing accelerometer pairs. There is a need for a theoretical framework to evaluate how these design variations, affect the expected performance of these devices

Three methods of design comparison will be presented: 1) Transformation of noise, a calculation of the degree of noise reduction produced by the method of transforming and combining measured gradient components. 2) Inversion errors, comparison of the degree to which noise induces errors in the values of parameters determined in a parametric inversion calculation. 3) Sensitivity, analysis of the response of each system to a point source and how that source varies as a function of location in 3D space. Each of these methods focuses on a different aspect of the practice of gravity gradiometry. Specifically, noise, inversion and source detection.

Analysis will be centered on comparison between the two gravity gradiometer designs manufactured by Lockheed-Martin. The full tensor gradiometer (FTG) and the horizontal partial tensor gradiometer that is part of the Falcon survey system. All three methods predict that in order for these two gradiometer designs to yield equivalent results the noise level of the horizontal partial tensor gradiometer must be less than that of each of the three sub-gradiometers of the FTG by a factor of 3.08.

Key words: Gravity, Gradiometer, Tensor, Inversion, Noise

INTRODUCTION

Current gravity gradiometers, both operating and under development, differ with respect to the number and orientation of their core gradient sensing components. Theoretical comparison of their capabilities requires a framework for assessing the effect of these differences on both signal strength and noise level. The approach given here is based on three aspects 1) Sensitivity: The ability to detect a given source, 2) Noise: The level of noise that remains after an optimal noise reduction process and 3) Inversion: The ability to solve for the source geology.

The signal due to geological sources is not uniformly distributed between gravity gradient components. Therefore some sensor orientations will detect stronger signal than others. This effect is modelled by consideration of sources that have simple geometries. The instrument sensitivity is defined as the total signal detected by the gradiometer. This is summed over all available channels and provides a means of comparing the predicted signal to noise level.

The underlying field equation makes it possible to calculate any component of the gravity gradient tensor from other components. This has obvious application to the mapping of components that have not been measured. It also has value as a means of noise reduction. If alternate versions of a gradient field can be calculated it is possible to generate a weighted average version of the field. This stacking process will generate a reduced noise product. The degree of noise reduction depends on the orientation of the raw gradient measurements. The resultant noise level provides a means of comparing gradiometer designs.

Any quantitative application of gravity gradiometry requires some form of inversion. The presence of noise will inevitably induce errors in the resulting model of the undersurface. A method based on analysis of parametric inversion will be given here. At least for this subset of inversion methods the relationship between gradiometer noise and inversion error can be quantified. As was the case both for sensitivity and noise, there is a non-trivial relationship between the geometry of the gradiometer design and its predicted performance.

METHODS

Gradiometer designs

Three gravity gradiometer designs will be considered here. The FTG, full tensor gradiometer, the horizontal gradiometer operated under the tradename Falcon and the partial tensor device under development with the tradename, HD-AGG.
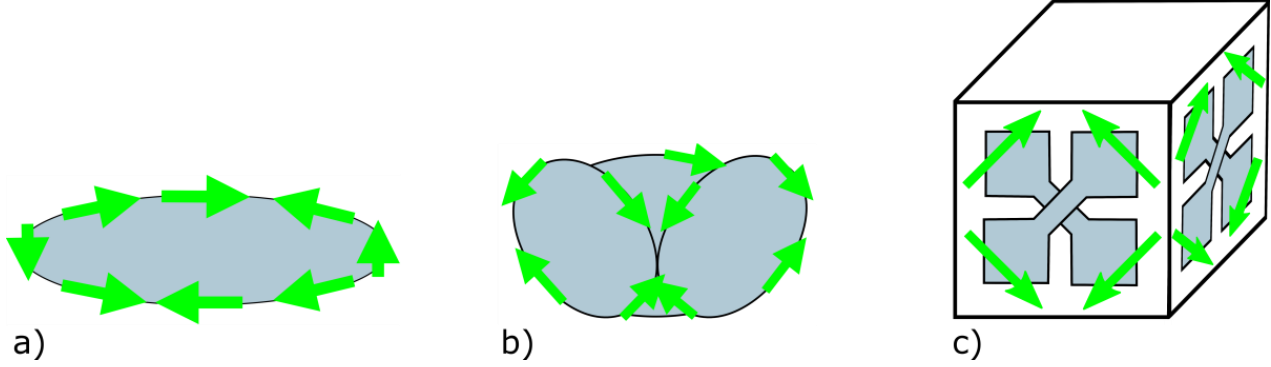

Figure 1: Schematic diagrams of the gravity gradiometer designs being compared. a) The horizontal partial tensor gradiometer (HPTG) that is part of the Falcon surveying system. It consists of 4 opposing pairs of tangentially oriented accelerometers in a single rotating assembly. It measures two gravity gradient components, Txy and Tuv=(Tyy-Txx)/2. b) The FTG, full tensor gradiometer. It consists of 3 sub-gradiometers each of which is a rotating assembly of 2 pairs of tangentially oriented accelerometers. It directly measures all components of the gradient tensor. c) The Gedex partial tensor gradiometer (GPTG) consists of 2, vertically oriented and mutually perpendicular, sensors that measure the differential torque of a double dumbbell mass arrangement. The green arrows represent the equivalent accelerometer orientation. The device measures two gradient components, (Tzz-Txx)/2 and (Tzz-Tyy)/2.

The FTG and Falcon horizontal partial tensor gradiometer (HPTG) are manifestations of the same rotating disk design invented by Lockheed-Martin (Hofmeyer, 1994). The core component of both is a rotor holding pairs of opposing tangentially oriented accelerometers. Four accelerometers, two perpendicular pairs are the minimum number required to make an accurate measurement. For such a quartet the gravity gradient is proportional to the sum of the accelerometer outputs. As the disk rotates so does the component sensed. Two distinct components can be recovered by demodulation of the output signal.

The HPTG (Lee, 2001) design uses 8 accelerometers on a single rotor oriented so as to turn about a vertical axis, Figure 1a. The two sensed gradient components are Txy and (Tyy-Txx)/2 (denoted as Tuv). The notation Tij indicates the derivative of the ith component of the gravity vector with respect to displacement in the jth direction. x-, y- and z- respectively denote the East-, North- and Down-directions.

The FTG (Jekeli, 1988) measures the full gradient tensor by using three mutually orthogonal rotating disk sub-gradiometers, Figure 1b. For reasons of symmetry they are mounted such that the rotor axes form an equal angle with the vertical. Each rotor measures two components of the gravity gradient, T_{ab} and $(T_{bb}-T_{aa})/2$ where a- and b- are perpendicular directions in the plane of the disk. These outputs are referred to as the inline and cross outputs of the sub-gradiometer. Every component of the gravity gradient tensor can be written as a linear combination of these six outputs and therefore can be considered to be directly measured.

The HD-AGG[tm] (Carrol et al 2010) is a partial tensor gradiometer developed by Gedex Systems Inc. So as to avoid using tradenames it will be referred to here as the GPTG to denote "Gedex Partial Tensor Gradiometer". It consists of two mutually perpendicular cryogenically cooled, cross-dumbbell gradiometers (Baker et al 2016), Figure 1c. Both are oriented about a horizontal axis such that their outputs are (Tzz-Txx)/2 and (Tzz-Tyy)/2. The sum of these output channels is (3/2) Tzz. Therefore this is a device that directly measures the most useful gradient component to interpret. The difference between output channels is (Tyy-Txx)/2, which is also one of the outputs of the HPTG. A similar device is also being developed at the University of Western Australia (Anstie et al 2009).

Each of the three methods given below makes use of the concept of balanced independent outputs. These are defined as a set of outputs scaled so as to show equal noise levels and arranged such that noise is uncorrelated between these channels. These are the raw outputs of the device written in purest form. For the HPTG these channels can be assumed to be Txy and (Tyy-Txx)/2. For the GPTG they are the gradient differences (Tzz-Txx)/2 and (Tzz-Tyy)/2. For the FTG the balanced outputs are the three inline and three cross sub-gradient outputs.

Sensitivity

Following Brewster (2016a) which is based on the work of Dransfield (2014), consider a survey intended to detect a point source located at (x,y,z). The total observation S_{obs} is given by

$$S_{obs}^2(x,y,z) = \sum_p \sum_i (g_{ip} + \nu_{ip})^2 \tag{1}$$

where g_{ip} is the signal observed in the ith output channel when the gradiometer is located at the pth observation location of the survey and η_{ip} is the noise present during that individual observation. First order noise terms average to zero in the expansion and we have

$$S^2_{obs}(x, y, z) = S^2_T(x, y, z) + \sigma^2_T$$

(2)

where σ_T is the total noise and S_T is the total instrument sensitivity given by

$$S_T = \sum_p \sum_i g^2_{ip}$$

(3)

If we consider that the signal to noise ratio can be written

$$S/N = \sqrt{\frac{S_T}{\sigma_T}}$$

(4)

it can be seen that calculation of the total sensitivity provides a means of comparing the signal to noise ratio that can be expected from gradiometers.

Noise

It is a property of solutions to the Laplace equation that expressions for the derivatives of the gravitational potential can be written in very compact form in Fourier-domain (Blakely, 1996)

$$\hat{T}_{ij} = s_{ij}\hat{\phi}$$

(5)

where phi is the gravitational potential and 'hat' denotes 2 dimensional Fourier transforms calculated on a horizontal plane. The differentiation functions, s_{ij}, are given by

$$
\begin{aligned}
s_{zz} &= k^2_z \\
s_{xx} &= -k^2_x \\
s_{yy} &= -k^2_y \\
s_{xz} &= ik_x k_z \\
s_{yz} &= ik_y k_z \\
s_{xy} &= -k_x k_y
\end{aligned}
$$

(6)

where kx and ky are the x- and y- components of wavenumber, kz is the vertical wavenumber given by

$$k^2_z = k^2_x + k^2_y$$

(7)

and i denotes the square root of -1.

Each of the gradiometer devices discussed here are such that gradient tensor components can be expressed as linear combinations of the raw output channels. We can write

$$T_a = \sum_b M_{ab} I_b$$

(8)

were T_a is the ath gradient component, I_b is b^{th} instrument output channel and M_{ab} is a matrix of coefficients describing the geometry of the sensor. It can be shown (Sanchez et al 2005, Brewster 2016b) that the optimum combination of components in Fourier domain is given by

$$\hat{\phi}' = \frac{\sum_a \sum_b |s_a| M_{ab} \hat{I}_b}{\sum_a |s_a|^2}$$

(9)

where the sum over 'a' includes only gradient components for which the value of T_a in Equation 8 is non-zero.

For the HPTG design it is advantageous to add a composite gradient component Tuv = (Tyy-Txx)/2. The matrix, M, consists of only 2 non-zero elements and Equation 9 becomes

$$\hat{\phi}'_{HPTG} = \frac{k_x k_y \hat{T}_{xy} + \frac{1}{2}(k_y^2 - k_x^2)\hat{T}_{uv}}{k_x^2 k_y^2 + \frac{1}{4}(k_y^2 - k_x^2)^2}$$

(10)

Likewise, for the GPTP gradiometer, two composite components are introduced, Tuw = (Tzz-Txx)/2 and Tvw = (Tzz-Tyy)/2. Equation 9 becomes

$$\hat{\phi}'_{VPTG} = \frac{\frac{1}{2}(k_x^2 + k_z^2)\hat{T}_{uw} + \frac{1}{2}(k_y^2 + k_z^2)\hat{T}_{vw}}{\frac{1}{4}(k_x^2 + k_z^2)^2 + \frac{1}{4}(k_y^2 + k_z^2)^2}$$

(11)

In the case of the FTG, M has only a few non-zero elements. This is because the components of gravity gradient sensed by the sub-gradiometers do not coincide with any components of the gradient tensor expressed in x, y, z coordinates. It has been found (Brewster 2016b) that the effect of this on the expression for the optimum sum is to adjust the weightings by constant coefficients

$$\hat{\phi}'_{FTG} = \frac{r_{zz}s_{zz}^* \hat{T}_{zz} + r_v s_{xz}^* \hat{T}_{xz} + r_v s_{yz}^* \hat{T}_{yz} + r_h s_{xy}^* \hat{T}_{xy} + r_h s_{uv}^* \hat{T}_{uv}}{r_{zz}|s_{zz}|^2 + r_v|s_{xz}|^2 + r_v|s_{yz}|^2 + r_h|s_{xy}|^2 + r_h|s_{uv}|^2}$$

(12)

where * denotes the complex conjugate. The values of the coefficients are, r_{zz}=0.67, r_v=1.15 and r_h=1.01.

Application of Parseval's theorem leads to an expression for the noise in each gradient component

$$\sigma^2(T_n) = \frac{1}{4\pi^2} \sum_b \int_{-\infty}^{+\infty} \int_{-\infty}^{+\infty} \left\| \frac{1}{\sum s_i^2} \right\|^4 \times \left\| I_b s_n \sum s_a^* M_{ab} \right\|^2 dk_x dk_y$$

(13)

Inversion

The relevant definition of inversion is any method that takes the observed data set and generates an estimate of the source distribution. This analysis is confined to the parametric inversion subset of inversion methods. The characteristics of the source distribution are described using a relatively small number of parameters. Inversion is now presented as a well overdetermined optimization problem and the parameters can be found with high certainty. Uncertainty in this family of inversion methods tends to reside in the initial choice of parameterization scheme.

Following Pilkington (2013) and Brewster (2017), a set of observations, T_j, are related to a set of parameters, a_i, that describe the source. The solution for the best fitting set of parameter values is found from the derivative of the gradient measurements with respect to changes in parameter values. When linearized this relationship is

$$\Delta T = M \Delta a$$

(14)

where M_{ij} is the Jacobian matrix of derivatives that describe the effect on the observed data of changing each parameter in turn

$$M_{ij} = \frac{\partial T_i}{\partial a_j}$$

(15)

If this can be solved to predict Δa from the gradiometer measurements the parameters of the source body can be adjusted iteratively. At each step the values of Δa guide the process until it converges.

One approach to this problem is to use Singular Value Decomposition to find the generalized inverse of matrix, M. It is factorized it as follows

$$M_{ij} = U \cdot s \cdot V^T$$

(16)

If there are p parameters and b observations, V is a b-by-b unitary matrix, U is a p-by-b matrix in which the columns of length p are normalized and orthogonal to one another. The b-by-b diagonal matrix, s contains the amplitudes needed to scale U. The diagonal values of s are the square roots of the eigenvalues of M. These properties of the factor matrices allow Equation 14 to be written

$$\Delta a = V \cdot s^{-1} \cdot U^T \cdot \Delta T \tag{17}$$

Partially dropping matrix notation and writing the matrix multiplications as an explicit sum over subscripts yields

$$\Delta a_i = \sum_j (V \cdot s^{-1} \cdot U^T)_{ij} \Delta T_j \tag{18}$$

If the parameterization is a good match to the true source geology the inversion process will iterate until the noise content of ΔT dominates over any residual signal. At this point the variance of a_i represents the degree of uncertainty in the final inversion result and is in simple proportion to the level of instrumental noise.

If there is no correlation between noise in the gradiometer signal channels and each has an equal noise level, the variances of the parameter estimations are given by

$$\sigma^2(a_i) = \eta^2 \sum_j (V \cdot s^{-1} \cdot U^T)^2_{ij} \tag{19}$$

where η is the gradiometer noise level.

Results

Sensitivity

Equation 3 is applied to the field from a spherically symmetric source. It is a useful limiting case to assume that observation points are plentiful, that is, tightly spaced relative to the depth of the center of the source. It is also useful to perform the sum in Equation 3 in order of distance from the center of source. This allows the sensitivity of the gradiometer to be calculated as a function of the width of the observation set.

The chart in Figure 2 shows cumulative values of the square root of the relative sensitivity as a function of observation radius. It is plotted relative to the sensitivity of the FTG device. The horizontal radius is defined as the distance between the observation point and the vertical line passing through the center of the source. Each point on the cumulative curve represents the relative sensitivity calculated using all observation points nearer to the center point than the given radius. The only distance scale in this scenario is defined by the depth of the source. The independent variable is chosen as radius/source depth with no loss of generality.
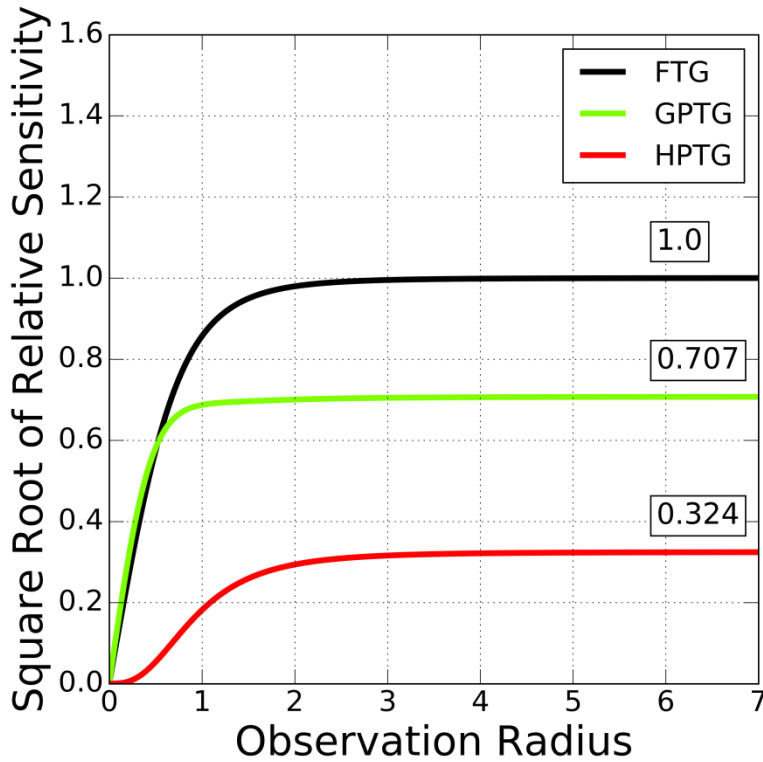
Figure 2: Square root of cumulative relative sensitivity plotted as a function of observation radius for three gradiometer designs. Each is plotted relative to the value for the FTG design in the limit of large observation radius. The numbers indicate the value that each curve tends toward as the observation radius becomes large.

The FTG and GPTG show similar sensitivity at small observation radius. The HPTG requires a larger observation set before it reaches its full sensitivity. At larger observation radius the FTG design has the largest sensitivity. with the GPTG and the HPTG lower by factors of square root of two and 3.08 respectively.

Noise

The expression for predicted noise given in Equation 13 was evaluated numerically for all three gradiometer designs. The results are shown in Table 1. For each gradient component the 'before' column contains the noise level before any noise reduction process. The 'after' column contains the noise level after processing using the Fourier-domain process described above. All noise levels are stated relative to those in the raw outputs of the gradient sensing components. These are noise amplitudes, that is, square root of variance, not the variance itself. For the HPTG and GPTG some gradient components are missing from the 'before' column and are only known once calculated during the noise reduction process.

	Tzz		**Txy**		**Tuv**		**Txz**		**Tyz**	
	before	after	before	after	before	after	before	after	before	after
FTG	1.155	0.657	0.944	0.233	0.944	0.233	0.882	0.465	0.882	0.465
HPTG	-	2	1	0.707	1	0.707	-	1.414	-	1.414
GPTG	0.943	0.918	-	0.325	0.707	0.325	-	0.650	-	0.650

Table 1: Predicted relative noise levels for the 3 gradiometer designs being compared. The 'before' column give the noise amplitude in the unprocessed gradient components given a noise amplitude of 1 in the raw output channels of the device. The 'after' column give the predicted noise amplitude after processing using an optimum combination of converted gradient components. A dash indicates that a gradient component is not directly measured by the gradiometer device. Noise amplitude is defined as the square root of the noise variance.

For the FTG the largest noise reduction, by a factor of 4.05, occurs in the Txy and Tuv components. Likewise, for the GPTG the largest noise reduction is in Tuv. For the Tzz component the GPTG only achieves a 2.6 % noise reduction. The gradients that it measures directly, Txy and Tuv, the HPTG achieves noise reduction by a factor of 2.83. Note that in the 'after' column the ratios Tzz/Txy = Tzz/Tuv = 2.83 (square root of 8) and Tzz/Txz = Tzz/Tyz = 1.41 (square root of 2) are the same for all three gradiometer designs.

Inversion

Equation 19 is applied to the case of inversion for the parameters describing a spherically symmetric source mass. Four parameters are required to completely describe this source, its mass and the three position coordinates of its center. As was the case when analyzing instrument sensitivity the observations are assumed to be sufficiently dense and are arranged in order of distance from the center of source.

The results are shown in Figure 3. The inversion error for each parameter is plotted relative to that calculated using the FTG and a wide observation radius. The errors in the two horizontal location coordinates were found to be very similar and so are pooled together into a single line.
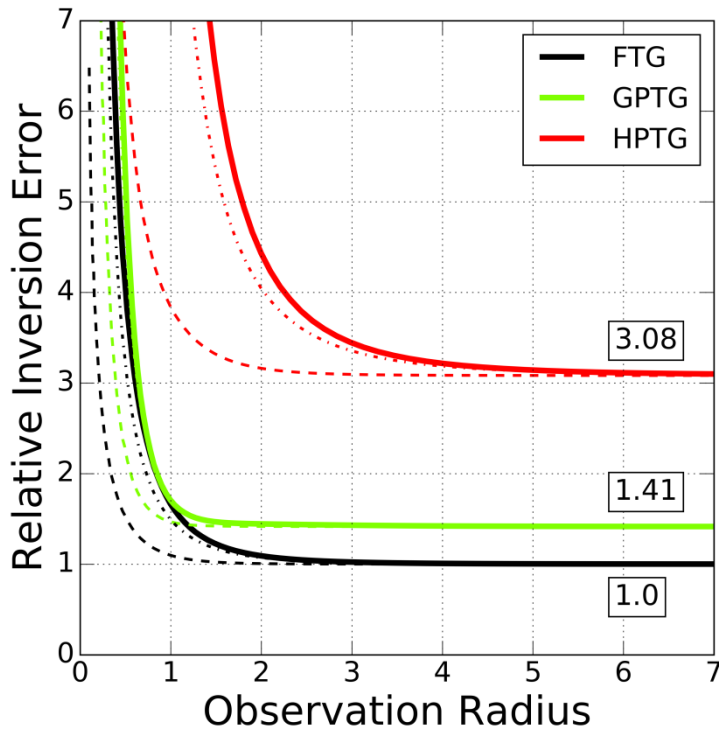

Figure 3: Relative inversion error plotted as a function of observation radius for three gradiometer designs. Each is plotted relative to the value for the FTG design in the limit of large observation radius. The numbers indicate the value that each curve tends toward as the observation radius becomes large. The solid lines indicate the mass error, lines with long dashes indicate the horizontal error and lines with short dashes indicate the vertical error.

As expected the error level is high if the observation radius is small. The HPTG requires a wider radius to reach the limiting error level. The exception being the horizontal position error. For small observation sets the FTG and GPTG show similar values before flattening out to different constant values. For large observation sets the relative inversion errors in the GPTG and HPTG are higher than those of the FTG by factors of square root of two and 3.08 respectively.

Discussion

Key ratios stand out among the results presented above because they have the same value in each of the three analyses. When comparing the FTG to the HTPG this ratio is 3.08. For the FTG to GPTG comparison the ratio is the square root of two, 1.41. For the sensitivity analysis these ratios are seen via their inverse in the results presented in Figure 2 and for inversion the ratios are clearly seen in the results shown in Figure 3. The equivalent ratios taken from the noise analysis differ by less than two percent. Comparison of values in the 'after' columns of Table 1 gives a ratio of 3.04 for the HPTG versus the FTG and 1.40 for the GPTG versus the FTG.

The implication of this is that for the HPTG to match the performance of the FTG the raw noise level of its gradient channels needs to be less than those of the FTG by a factor of 3.08. Likewise, the raw noise level in the outputs of the GPTG need to be less by a factor of 1.41 to match the FTG.

As the FTG and HPTG have many design features in common and are made by the same manufacturer it is possible to estimate their relative raw noise levels. Due to more sensors being placed on a similar stabilized platform, the sub-gradiometers of the FTG are of necessity smaller than the single gradiometer of the HPTG. The larger rotor also hosts twice as many accelerometer pairs. Given the target ratio of 3.08 a break-even diameter can be estimated for the HPTG as being 2.17 times that of the FTG rotors (Brewster 2016a). This is under the assumption that accelerometers are the dominant source of noise and that noise in different pairs of accelerometers can be assumed to be uncorrelated. The actual dimensions of these components is Lockheed Martin proprietary information but an estimate of 'about 2' has been previously published (Dransfield, 2007)

The gradiometer designs that directly measure Tzz, FTG and GPTG perform relatively better than the HPTG when directly over the source. The HPTG can be thought of as a side-looking device as it has zero sensitivity to sources directly below it. The importance of this aspect is somewhat lessened in airborne surveying because even if a flight line passes directly over a source, significant portions of that line will still be located such that the source is at a more favorable angle to be detected.

Any quantitative conclusion from this analysis is relative to the raw noise level of the instrument. It can tell us nothing about how the gradiometer will perform under particular conditions such as high vertical acceleration. What it does give is a means of evaluating how much affect this noise will have on the final product.

Conclusion

Three methods have been presented for the analysis of gradiometer designs. These involve consideration of: Sensitivity, the degree of noise reduction and the magnitude of inversion errors. Each of these represent a method of quantifying the degree to which noise in its raw outputs affects the utility of a gradiometer.

Three gradiometer designs have been analysed by these methods: The FTG, the two horizontal component gradiometer that is part of the Falcon surveying system (HPTG) and the two component gradiometer currently under development by Gedex Inc. (GPTG).

Each method produced similar quantitative results. In order to match the performance of the FTG design the raw noise level of the HPTG must be lower by a factor of 3.08. This is a comparison between the two raw output channels of the HPTG and the six output channels of the FTG. For the GPTG the equivalent factor is 1.41 (the square root of two). This quantifies the advantage the FTG has over the other two designs due to the number and orientation of its sensors.

References

Anstie, J., Aravanis, T., Haederle, M., Mann, A., McIntosh, S., Smith, R., Van Kann, F., Wells, G., Winterflood, J., 2009, Vk-1-a new generation airborne gravity gradiometer: ASEG Extended Abstracts, no. 1: 1-5.

Baker, K., Carroll, K.A., Dickson, B., Hatch D., Main, B., McTavish, D., Pefhany, S., Sincarsin, G., Sincarsin, W., Sinton, J., Tomski, I., Wong, H., 2017, Advances in Airborne Gravity Gradiometry at Gedex: KEGS Symposium, Innovation and New Methods in Geophysics, Toronto, Canada, March 4th.

Blakely, R.J., 1996, Potential theory in gravity and magnetic applications: Cambridge University Press.

Brewster, J.R., 2016, Comparison of gravity gradiometer designs using the 3D sensitivity function. In SEG Technical Program Expanded Abstracts, Society of Exploration Geophysicists.

Brewster J.R., 2016, Reducing noise by transforming and combining gravity gradient components, In Airborne Gravity 2016– Abstracts from the ASEG-PESA Airborne Gravity 2016 Workshop, Geoscience Australia Record.

Brewster, J.R., 2017, Gravity gradiometer design comparison by analysis of parametric inversion: In SEG Technical Program Expanded Abstracts, Society of Exploration Geophysicists.

Carroll, K.A., Hatch, D., and Main, B., 2010, Performance of the Gedex high-definition gravity gradiometer: Airborne Gravity 2010-Abstracts from the ASEG-PESA Airborne Gravity Workshop: Published jointly by Geoscience Australia and the Geological Survey of New South Wales, Geoscience Australia Record 2010/23 and GSNSW File GS2010/0457, pp. 37-43.

Dransfield, M., 2014, Searchlights for gravity and magnetics: Geophysics 80, no. 1: G27-G34.

Dransfield, M., 2007, Airborne gravity gradiometry in the search for mineral deposits: In Proceedings of exploration, vol. 7, pp. 341-354.

Hofmeyer, G.M., and Affleck, C.A., 1994, Rotating accelerometer gradiometer: U.S. Patent 5,357,802, issued October 25, 1994.

Jekeli, C., 1988, The gravity gradiometer survey system (GGSS): Eos 69, no. 8.

Lee, J.B., 2001, FALCON gravity gradiometer technology: Exploration Geophysics 32, no. 3/4: 247-250.

Pilkington, M., 2013, Evaluating the utility of gravity gradient tensor components: Geophysics 79, no. 1: G1-G14.

Sanchez, V., Sinex, D., Li, Y., Nabighian, M., Wright, D., and vonG Smith, D., 2005, Processing and inversion of magnetic gradient tensor data for UXO applications: In 18th EEGS Symposium on the Application of Geophysics to Engineering and Environmental Problems.